ACS OMEGA

http://pubs.acs.org/journal/acsodf

Article

Unroasted Green Coffee Extract-Loaded Solid Lipid Nanoparticles for Enhancing Intestinal Permeation

Yomna A. Moussa, Mahmoud H. Teaima, Dalia Attia,* Mohey M. Elmazar, and Mohamed A. El-Nabarawi

Cite This: *ACS Omega* 2023, 8, 20251−20261

Read Online

ACCESS | Metrics & More | Article Recommendations | Supporting Information

ABSTRACT: Green coffee bean extract (GCBE) provides diversified health benefits. However, its reported low bioavailability impeded its utilization in various applications. In this study, GCBE-loaded solid lipid nanoparticles (SLNs) were prepared to improve the bioavailability through enhanced intestinal absorption of GCBE. During the preparation of promising GCBE-loaded SLNs, the lipid concentration, surfactant concentration, and co-surfactant amount are crucial that were optimized using the Box−Behnken design, while particle size, polydispersity index (PDI), ζ-potential, entrapment efficiency, and cumulative drug release were the measured responses. GCBE-SLNs were successfully developed by a high shear homogenization technique using geleol as a solid lipid, tween 80 as a surfactant, and propylene glycol as Co-SAA. The optimized SLNs contained 5.8% geleol, 5.9% tween 80, and 80.4 mg PG resulting in a small particle size of 235.7 ± 12.5 nm, reasonably acceptable PDI of 0.417 ± 0.023, and ζ-potential of −15 ± 0.14 mV, with a high entrapment efficiency of 58.3 ± 0.85% and cumulative release of 7575 ± 0.78%. Furthermore, the performance of the optimized GCBE-SLN was evaluated using an ex vivo everted sac model where the intestinal permeation of GCBE was improved due to nanoencapsulation using SLN. Consequently, the results enlightened the auspicious potential of exploiting oral GCBE-SLNs for boosting intestinal absorption of chlorogenic acid.

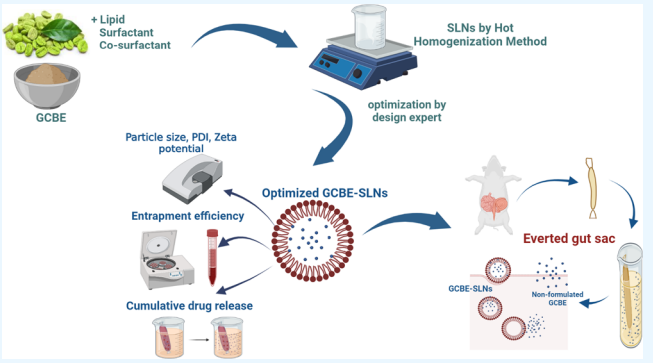

INTRODUCTION

Green coffee bean extract (GCBE) has been proven to possess various therapeutic effects, including antioxidant,[1] weight management,[2] and antiproliferative activity.[3] The therapeutic effects of GCBE are primarily attributable to chlorogenic acid (CGA), a polyphenol antioxidant found as the dominant phyto-constituent in green coffee. GCBE was preferred without roasting or fermentation to attain high levels of CGA, which is reduced during the roasting process.[4]

The most prevalent indication of GCBE is weight management.[5] Weight loss is a long-standing objective that requires an effective and safe remedy. In this regard, GCBE offers the appealing privilege of being a natural supplement with negligible side effects.[6] The aptness and efficiency of GCBE in weight management have been exhaustively discussed in previous studies that provided accumulating evidence regarding the auspicious utilization of GCBE as an anti-obesity supplement in animals and clinical studies.[2,4,5,7]

Upon absorption of GCBE from the intestine,[8] GCBE may attain its anti-obesity effect by several mechanisms. These mechanisms include accelerating lipolysis, suppressing lipogenesis, restraining the accumulation of hepatic triglycerides, and changing adipokine plasma levels and body fat distribution. In addition, GCBE may cause upregulation of fatty acid oxidation and peroxisome proliferator-activated receptor alpha expression in the liver and downregulation of fatty acid and cholesterol biosynthesis.[9,10]

Although GCBE has high therapeutic efficiency, its poor oral bioavailability and limited absorption significantly reduced its utilization like many other natural products.[11] Previous animal studies showed that only one-third of CGA managed to enter the bloodstream after oral consumption and was rapidly metabolized. According to Feng et al.,[12] this could be due to the hydrophilic nature of CGA that makes it challenging to cross physiological barriers, resulting in low drug bioavailability. Moreover, Mortelé et al.[13] investigated CGA's oral absorption and reported an overall limited intestinal absorption that involves an active efflux mechanism that results in low bioavailability of CGA. Generally, various pumps in the intestinal epithelium contribute to intestinal permeation. One type of pump, called an influx transporter, transfers the

Received: October 14, 2022
Accepted: May 23, 2023
Published: June 1, 2023

drug from the mucosal side to the serosal side. In contrast, a different kind of pump that lower CGA absorption called an efflux transporter operates oppositely by transporting the drug from the serosal side to the intestinal mucosa.[14]

Based on the premise mentioned above, a suitable delivery system for GCBE was necessitated to enhance the intestinal permeation of its CGA content and consequently improve its bioavailability. Over the past few years, nanoparticles have been attracting considerable research attention because of their outstanding properties.[15] Among eminent prevalent nanoparticles, solid lipid nanoparticles (SLNs) have been featured with unique potentials compared to traditional emulsions owing to their effectiveness in penetrating lipophilic barriers because of their small size.[16,17] In addition, the nano-sized particles offer a larger contact surface area for adherence to the intestinal wall, which can enhance absorption, increase bioavailability, and reduce systemic side effects.[18−20]

Moreover, compared to other types of nanoparticles, SLNs proved lower production cost, higher stability, better protection of the encapsulated bioactive compound, and prolonged release compared to liposomes and niosomes, as well as better safety compared to polymeric nanoparticles, which encouraged SLN suitability for oral delivery.[17,21] Furthermore, SLNs are commonly recognized as safe oral drug delivery systems because of their basic composition of physiologically biodegradable and biocompatible lipids and the avoidance of organic solvents in the preparation method.[20]

Jointly, the above-mentioned merits may grant immense potential to SLNs as excellent candidates for enhancing intestinal permeation and absorption of GCBE. As so far, the data on the use of nanoparticles to improve the oral bioavailability of GCBE are inconclusive. Therefore, our hypothesis was that loading GCBE in SLNs would enhance GCBE intestinal absorption and consequently improve its oral bioavailability compared to free GCBE. In this study, an optimized GCBE-SLN was obtained using the Box−Behnken design (BBD). Then, its intestinal absorption was assessed using the everted gut sac model compared to free GCBE.

MATERIALS AND METHODS

Materials. GCBE was purchased from Biofinest (USA). Geleol (glyceryl monostearate) was generously donated by Gattefossé (saint-priest Cedex, France). Propylene glycol was purchased from Alpha Chemika (Mumbai, India). Tween 80 was obtained from AlNasr Pharmaceutical Chemicals Co. (Cairo, Egypt). Disodium hydrogen phosphate and potassium dihydrogen phosphate were obtained from Fischer Scientific, Acros Organic. The cellulose dialysis tubing membrane (molecular weight cutoff 12 kDa) was purchased from Sigma-Aldrich (St. Louis, MO, USA). All other chemicals used were of analytical grade.

Methods. *Construction of the Study Design.* BBD was used to study the influence(s) of GCBE-SLNs composition on its characteristics, including particle size (nm; Y1), polydispersity index (PDI) (Y2), ζ-potential (mV; Y3), entrapment efficiency (%; Y4), and cumulative drug released (%, Y5), while the explored independent variables, namely, lipid concentration (% w/w; X1), surfactant concentration (% w/w; X2), and Co-SAA amount (mg; X3), were studied at three levels, as shown in Table 1. Fifteen experimental runs, including three center points, were obtained using Design-Expert software version 11 and were indiscriminately prepared. The factor coding and layout of the experimental design are illustrated in Table 2. After developing the experimental formulations, model statistics and equations of responses were generated.

Table 1. Levels and Constraints of Independent and Dependent Variables

		levels		
code	independent variable	high	center point	low
X1	lipid concentration (% w/w)	6%	4.5%	3%
X2	surfactant concentration (% w/w)	7%	5%	3%
X3	Co-SAA amount (mg)	100 mg	62.5 mg	25 mg
code	dependent variable	constraints		
Y1	particle size (nm)	minimize		
Y2	PDI	minimize		
Y3	ζ-potential (mV)	maximize		
Y4	entrapment efficiency (%)	maximize		
Y5	cumulative drug release (%)	maximize		

Preparation of GCBE-Loaded Solid Lipid Nanoparticles. The fifteen suggested GCBE-SLNs formulae (Table 2) were synthesized as reported previously by Patel and Sawant[22] with slight modifications using the hot shear homogenization technique followed by ultra-sonication. Briefly, according to the design, specified amounts of tween 80 (surfactant) and propylene glycol (Co-SAA) were dissolved in deionized water to develop 25 g of the aqueous phase. In contrast, GCBE (35 mg) was dispersed in geleol to form the lipid phase. Both aqueous and lipid phases were pre-heated at 70 ± 1 °C. Afterward, the aqueous phase was poured into the lipid phase and mixed using a magnetic stirrer at 1000 ± 5 rpm to form a coarse emulsion, followed by ultra-sonication using a probe sonicator (Vibra-Cell VCX130; Sonics, CT, USA) at 100% amplitude in an ice bath for 10 min. The formed emulsion was kept at room temperature (25 ± 1 °C) for 1 h to obtain the SLNs and then stored in tightly closed containers at 4 °C and subsequently subjected to further characterization.

Characterization of GCBE-Loaded SLNs (Observed Responses). *Particle Size (Y1), Polydispersity Index (PDI) (Y2), and ζ-Potential (Y3).* The average particle size, size distribution, and ζ-potential of all prepared GCBE-SLNs were measured by the dynamic light scattering technique using Malvern Zetasizer (Nano-ZS Malvern Instrument, UK). GCBE-SLNs dispersions were diluted by deionized water to obtain the optimum count rate (kcps). The dispersions were then sonicated for 2 min preceding analysis using a bath sonicator to guarantee proper scattering intensity. The measurements were carried out at an equilibrated room temperature of 25 ± 1 °C. In addition, ζ-potential was determined using a DTS 1060C zeta cuvette at 25 ± 1 °C and 78.5 dispersant dielectric constants.[23] Measurements were carried out in triplicates, and results were mentioned as average ± standard deviation (SD).

Entrapment Efficiency (EE%) (Y4). The EE% of the developed GCBE-SLNs was measured using the indirect method.[24] Dispersions of GCBE-SLNs were diluted with distilled water and centrifuged by a cooling centrifuge (Sigma 2−16 KL, Germany) for 2 h at 4 °C and 12,000 rpm. After that, the concentration of free GCBE was determined using a UV−vis spectrophotometer (V-630, Jasco, Tokyo, Japan) at λ_{max} (324 nm) as determined in the scanning spectrum (Figure S1 in the Supporting Information). The entrapment efficiency

https://doi.org/10.1021/acsomega.2c06629
ACS Omega 2023, 8, 20251−20261

Table 2. Layout of Experimental Design and the Observed Responses[a]

code	X1	X2	X3	Y1[b]	Y2[b]	Y3[b]	Y4[b]	Y5[b]
F1	6.00	3.00	62.50	318.2 ± 8.79	0.626 ± 0.09	−20.3 ± 0.07	37.7 ± 0.49	67.0 ± 6.36
F2	3.00	5.00	100.00	232.6 ± 25.68	0.670 ± 0.01	−14.7 ± 0.42	24.4 ± 0.97	74.9 ± 5.00
F3	3.00	7.00	62.50	190.4 ± 2.17	0.777 ± 0.04	−13.9 ± 2.33	7.9 ± 1.33	100.0 ± 3.54
F4	6.00	5.00	100.00	237.2 ± 29.51	0.296 ± 0.15	−13.4 ± 0.35	50.0 ± 0.80	71.5 ± 6.03
F5	4.50	7.00	100.00	195 ± 9.17	0.534 ± 0.08	−05.0 ± 0.54	39.7 ± 1.91	89.0 ± 7.78
F6	4.50	7.00	25.00	223 ± 30.69	0.473 ± 0.01	−16.6 ± 0.57	29.9 ± 1.29	74.0 ± 9.90
F7	3.00	5.00	25.00	278.6 ± 31.82	0.244 ± 0.10	−24.4 ± 0.21	35.4 ± 0.65	88.7 ± 10.36
F8	6.00	7.00	62.50	222.5 ± 21.30	0.434 ± 0.003	−13.2 ± 0.64	57.3 ± 4.36	61.2 ± 4.83
F9	4.50	5.00	62.50	271.9 ± 6.22	0.554 ± 0.06	−20.1 ± 0.57	52.5 ± 0.67	97.9 ± 1.51
F10	4.50	5.00	62.50	249.6 ± 29.25	0.611 ± 0.04	−21.8 ± 0.21	68.2 ± 2.35	82.0 ± 5.65
F11	4.50	5.00	62.50	251 ± 31.06	0.417 ± 0.05	−21.9 ± 1.20	55.6 ± 0.66	83.6 ± 3.24
F12	3.00	3.00	62.50	280.8 ± 3.01	0.474 ± 0.02	−23.5 ± 1.41	64.9 ± 0.11	63.0 ± 3.53
F13	6.00	5.00	25.00	278.6 ± 7.73	0.514 ± 0.02	−19.5 ± 2.05	20.5 ± 0.26	46.0 ± 7.80
F14	4.50	3.00	100.00	310.3 ± 9.10	0.640 ± 0.10	−19.7 ± 0.28	57.5 ± 0.15	55.4 ± 6.10
F15	4.50	3.00	25.00	295.3 ± 16.33	0.421 ± 0.02	−18.7 ± 0.85	35.0 ± 4.66	75.3 ± 3.75

[a]Abbreviations: X1, lipid concentration (% w/w); X2, surfactant concentration (% w/w); X3, Co-SAA amount (mg), Y1, particle size; Y2, polydispersity index; Y3, ζ-potential; Y4, entrapment efficiency %; Y5, cumulative drug release %. [b]Values are reported as mean ± SD.

of GCBE in SLNs was determined using the following equation:[24]

$$\text{EE}\ (\%) = (\text{total drug content} - \text{drug content in the supernatant})/\text{total drug content} \times 100 \quad (1)$$

In Vitro Cumulative Drug Release (Y5). Cumulative amounts of GCBE released from SLNs dispersions were measured for 24 h using the cellulose dialysis bags technique.[25] GCBE-SLNs dispersions (0.5 mL) were put in 7 cm cellulose bags (molecular weight cutoff 12 kDa) and sealed using thread, then transferred to beakers containing 100 mL phosphate buffer solution (pH = 7.4). Beakers were shaken horizontally in a shaking water bath (WSB-18, Daihan Scientific Co. Ltd., Gangwon-do, Korea) for 24 h at 37 ± 1 °C and 100 rpm. At definite time intervals (1, 2, 3, 4, 5, 6, and 24 h), a 2 mL sample of the medium was withdrawn and then substituted with an equal volume of the respective fresh medium to maintain sink condition. The drug content of the samples was measured using a UV−vis spectrophotometer at λ_{max} 324 nm. The release profile of GCBE-loaded SLNs was compared with free extract solution of the same concentration and analyzed to decide the best fit kinetic model. All experiments were implemented in triplicates, and results were exhibited as average value ± SD.

Selection of the Optimized Formula of GCBE-SLNs. The best achievable GCBE-SLNs dispersion was numerically deduced by Design-Expert Software using the statistical optimization of the 15 GCBE-SLNs formulations. A desirability function was used to optimize the tested input parameters to achieve the constraints illustrated in Table 1. The optimized formula was selected to fulfill the highest desirability and sought-after responses. Subsequently, the optimized formula of SLNs was prepared and evaluated for its particle size, PDI, ζ-potential, entrapment efficiency, and cumulative drug release using the previously mentioned techniques to assert model durability. The model accuracy and reliability were also ensured by comparing the observed values of the responses under study to the predicted ones and then calculating the residual error.

Transmission Electron Microscope (TEM). The surface morphology and shape of the optimized formula of GCBE-SLNs were visualized using a transmission electron microscope (model JEM-2100, Jeol, U.S.A.). A sample of optimized GCBE-SLNs was diluted using deionized water then one drop of the dispersion was placed on a carbon-coated copper grid. The sample was stained using 2% w/v uranyl acetate solution. Afterward, grids were air dried at 25 ± 1 °C preparatory to the microscopic investigation.[26]

Ex Vivo Intestinal Permeation Study on Optimized GCBE-SLNs Using the Everted Gut Sac Model. Intestinal permeation of optimized GCBE-SLNs dispersion and non-formulated extract solution was evaluated using everted gut sac technique as described previously.[27] Kreb's Ringer phosphate bicarbonate buffer (KRPB) (pH 7.4) was prepared according to Schilling & Mitra[28] with some modifications. Intestinal sacs were obtained from healthy male rats (weighing 200−300 g) and starved for 20 h prior to the experiment. Intestinal sacs were obtained by midline incision of the rat's abdomen. The intestine was flushed with KRPB buffer solution several times. Then, divided into segments (7 cm each), it was gently everted over a steel rod. One end of the everted intestine was clamped and tied with a braided silk suture and then filled with 0.5 mL of KRPB buffer solution at 37 ± 1 °C. The filled intestine sacs were sealed at the other end with a second tie and then transferred to oxygenated incubation tubes filled with 10 mL of KRPB buffer solution containing a known amount of the optimized GCBE-SLNs or non-formulated GCBE. Sacs were removed and dried at the defined time intervals (30 and 60 min). The sacs were cut, and the fluids were drained into small eppendorfs and centrifuged for 20 min to remove any intestinal deposits.[29] Then, CGA was quantified by a previously developed and validated high-performance liquid chromatography (HPLC) method using a diode array detector (SPD-20 A, Shimadzu, Japan). Samples were eluted through a C_{18} column (Inertsil ODS-3, 5 μm, 4.6 × 250 mm^2). A gradient elution system was used with two mobile phases. Mobile phase (A) consisted of 0.1% formic acid in water. Mobile phase (B) was made of 0.1 formic acid in acetonitrile. Mobile phases were degassed and filtered prior to analysis. The analysis was performed at λ_{max} 324 nm with an injection volume of 10 μL and a flow rate of 1.0 mL/min.[30] The HPLC method was validated in terms of linearity, the limit of detection (LOD), and the limit of quantification (LOQ). All

https://doi.org/10.1021/acsomega.2c06629
ACS Omega 2023, 8, 20251−20261

Table 3. Analysis of Variance and Fit Statistics of the Responses[a]

	Y1		Y2		Y3		Y4		Y5	
independent variable	coefficient estimate	*p*-value	coefficient estimate	*p*-value	coefficient estimate	*p*-value	coefficient estimate	*p*-value	coefficient estimate	*p*-value
X1	9.26	0.0812	−0.0369	0.1993	−1.27	0.0224[b]	4.11	0.1286	−10.12	0.0065[b]
X2	−46.71	<0.0001[b]	0.0071	0.7866	−4.19	0.0001[b]	−7.56	0.0204[b]	7.94	0.0169[b]
X3	−12.55	0.0247[b]	0.0610	0.0582	−3.29	0.0004[b]	6.34	0.0378[b]	0.8538	0.7206
X1X2			−0.1237	0.0171[b]	0.6250	0.3074	19.13	0.0019[b]	−10.71	0.0202[b]
X1X3			−0.1610	0.0060[b]	0.9125	0.1581	10.12	0.0249[b]	9.80	0.0278[b]
X2X3			−0.0395	0.3137	−3.15	0.0023[b]	−3.19	0.3650	8.73	0.0410[b]
$X1^2$			−0.0178	0.6484	−0.2771	0.6489	−12.39	0.0136[b]	−9.09	0.0409[b]
$X2^2$			0.0682	0.1223	−3.26	0.0023[b]	−4.44	0.2402	−5.94	0.1338
$X3^2$			−0.0785	0.0854	−3.00	0.0033[b]	−13.80	0.0089[b]	−8.46	0.0513
R^2	0.9045		0.9116		0.9831		0.9517		0.9381	
adeq. precision	16.82		8.67		21.64		10.22		9.99	

[a]Abbreviations: Y1, particle size; Y2, polydispersity index (PDI); Y3, ζ-potential; Y4, entrapment efficiency %; Y5, cumulative drug release %; X1, lipid concentration; X2, surfactant concentration; X3, Co-SAA amount; R^2, *R*-squared; Std Dev.; standard error of the estimate. [b]Significant effect of factor ($p < 0.05$).

measurements were carried out in triplicates, and results were expressed as mean ± SD.

Statistical Analysis. All parameters obtained from the experiments were reported as average ± SD. Statistical analyses of responses using a one-way analysis of variance test (ANOVA) were provided by Design-Expert Software (Design Expert version 11.0.0 software, Stat-Ease, Inc., USA), while two-way ANOVA and unpaired *t* tests were performed using GraphPad Prism software (GraphPad version 9, CA, USA). Parameters with a *p*-value <0.05 were believed to be statistically significant.

RESULTS AND DISCUSSION

The GCBE-loaded SLNs were felicitously developed using the high shear homogenization technique. Such a method was reported to have appealing privileges, including short production times, ease of production, and organic solvent-free operation.[31] Response surface methodology was utilized to estimate the prominence of formulation-related determinants relative to SLNs characteristics. In view of this, the BBD was constructed to study the impact of independent variables' levels on the physicochemical attributes of the prepared SLNs. The independent variables and their levels were selected based on our pre-optimization study (unpublished). Particle size (nm; Y1), PDI (Y2), ζ-potential (mV; Y3), EE (%; Y4), and R (%; Y5) were opted as responses for 15 runs of SLNs loading GCBE, as illustrated in Table 2. The 15 runs included 3 center points as it's recommended to have center point replicates to assure that the design gives an accurate test of lack of fit and provides a proper estimate of an experimental error.[32] Based on our previous work (unpublished), GCBE was incorporated into SLNs at a fixed concentration (1.4 mg/mL) in all formulations. In contrast, the concentrations of geleol (X1), tween 80 (X2), and Co-SAA amount (X3) varied based on the design.

Moreover, statistical evaluations such as ANOVA, multiple correlation coefficients (R^2) tests, and lack-of-fit tests are provided by Design-Expert Software to determine the significance of the model, as illustrated in Table 3. All responses fitted the quadratic model except for the particle size, which showed a linear model. In addition, the correlation coefficient (R^2) values were detected, with all responses reflecting a good fit by the significant models. It is worth pointing out that the predicted R^2 and adjusted R^2 were in reasonable agreement for all response parameters with a difference of less than 0.2.[33] Adequate precision measures the signal-to-noise ratio where values greater than 4 indicate adequate signal. The fulfilled adequate precision (4) for the five achieved responses proves the capability of the reliable models to successfully navigate the design space.[34] The significance of models and the relative leverage of the studied variables on different responses are listed in Table 3. All models showed an insignificant lack of fit (*p*-value >0.1), which is preferable to ensure that a model fits the corresponding response well.[32]

Influence of Investigated Parameters on Particle Size (Y1) and PDI (Y2). The size of nanoparticles is fundamental to expect their leverage on bio-distribution, clearance, and, therefore, their characteristics and function. The spectacularly small size of SLNs offers promising potential regarding absorption, permeability, and bioavailability.[32] GCBE-SLNs were successfully prepared in a size range from 190.4 ± 2.17 to 318.2 ± 8.79, as illustrated in Table 2. The coefficient estimate represents the expected change in response per unit change in factor value when all other parameters are kept constant. Both surfactant concentration (X2) and Co-SAA amount (X3) had significant impacts on particle size ($p < 0.05$).

The negative coefficient estimate of X2 indicates an antagonistic relationship with particle size. Thus, as the surfactant concentration increases, the particle size decrease. This finding could be explained by the reduction of surface tension and surface free energy of the formulations produced because of the high shearing conditions during preparation, which reduces the particle size.[35] Furthermore, higher concentrations of surfactants achieve more stability in smaller lipid droplets and prevent their coalescing into larger droplets, as reported by Shah.[36]

As highly demonstrated in F12 versus F3, at a constant lipid concentration of 3% and Co-SAA amount of 62.5 mg, the particle size of SLNs distinctly reduced from 280.8 ± 3.01 to 190.4 ± 2.17 nm (the smallest attainable particle size in this study) as the surfactant concentration increased from 3 to 7%.

Similarly, the Co-SAA amount (X3) had a negative coefficient estimate, suggesting an indirect relationship with the particle size that can be justified by lowering the interfacial tension between the aqueous and lipid phase upon increasing

https://doi.org/10.1021/acsomega.2c06629
ACS Omega 2023, 8, 20251−20261

the Co-SAA amount. In addition, according to Badawi et al.,[37] as the Co-SAA amount increases, the particle size decreases due to the reduction in the formation of aggregations of lipid particles and the facilitated partition of the particles during homogenization, thus resulting in a higher surface area and smaller particle size. By the same token, it's evident in F7 versus F2 that when the CO-SAA amount increased from 25 to 100 mg at fixed lipid concentration (3%) and SAA concentration (5%), the particle size noticeably decreased from 278.6 ± 31.82 to 232.6 ± 25.68 nm.

Moreover, solid lipid concentration (X1) had an insignificant influence on particle size. Its positive coefficient estimate indicates a synergistic effect on the particle size. This behavior could be attributed to the high viscosity of the dispersion upon increasing the lipid concentration. That affects the homogenization efficiency through the initial emulsification phase and increases the collision of SLNs, which may cause aggregations.[35] As evidenced earlier, the results indicated that a high concentration of lipid contributed to building the particle size since by increasing lipid concentration, the surfactant may have a limited effect on reducing the particle size.[38] Moreover, another reason for this finding is the less efficient distribution of sonication energy in viscous dispersions resulting in a subsequent increase in particle size.[22]

Moreover, Emami et al.[39] reported that the nanoparticles' size strongly relies on the lipid concentration concerning the lipid's propensity to agglomerate when the concentration of lipid increases. It is noteworthy that, consistent with the explanations mentioned above, the largest attainable particle size was 318.2 ± 8.79 nm (F1), which is composed of the highest lipid concentration (6%) and the lowest SAA concentration (3%). In contrast, the least attainable particle size (190.4 ± 2.17) was obtained by F3, which contains the lowest lipid concentration (3%) and the highest surfactant concentration (7%).

With respect to particle size distribution characterization, PDI is a parameter used to define the size range of the lipidic nanocarrier systems. The PDI value is used to illustrate the monodispersed and polydispersed nature of nanoparticles. The higher the PDI value, the wider the droplet size distribution.[40] PDI offers an indication of the size uniformity of the dispersions. Scrutinizing nanoparticles' composition and processing are critical for obtaining low-scaled values of PDI <0.5.[41] As shown in Table 2, GCBE-SLNs formulations displayed fairly plausible values of PDI in the range from 0.244 ± 0.10 to 0.777 ± 0.04. ANOVA results showed that the model terms X1X2 and X1X3 had significant effects on PDI, representing the effect of the interaction of two spontaneously changed independent variables on PDI. Both X1X2 and X1X3 had an indirect relationship with the PDI, which could be explained that increasing the interaction between the lipid and the surfactant or Co-SAA will result in reducing the PDI due to formation of a more homogenous preparation. As commonly, increasing the surfactant or Co-SAA has a role in increasing the homogeneity of the size and formation monodisperse systems, which in our case was highly emphasized when interacted with lipid.[42]

Influence of Investigated Parameters on ζ-Potential (Y3). ζ-potential is an electric potential created because of the charges present on the surface of the particle. ζ-potential can be considered a stability indicating tool as it predicts the repulsion degree among similarly charged nanoparticles within the formulation.[43] This repulsive force prevents the particles' aggregation upon storage. Thus, ζ-potential indicates the degree of the physical stability of the formulation.[36] As illustrated in Table 2, all the GCBE-SLN formulations had a negatively charged ζ-potential ranging from −5 ± 0.54 to −24.4 ± 0.21 mV. The negative values of ζ-potential can be explained by the negative charge on the surface of SLNs that originated from residues of the fatty acids present in the prepared formulae.[39] Moreover, according to Scioli Montoto et al.,[44] lipid nanoparticles based on materials such as tween 80 tend to possess slightly or moderately negative charge in the range from −3 to −30 mV, which agrees with our results. Our findings agreed with the results obtained by Tan et al.[45] As shown in Table 3, X1, X2, X3, X2X3, $X2^2$, and $X3^2$ showed significant impact on ζ-potential (p-value <0.05). All three main independent variables (X1, X2, and X3) showed a negative antagonistic effect on ζ-potential, where the independent increase in each variable while maintaining other variables constant results in a significant decrease in ζ-potential. Moreover, ANOVA indicated that surfactant concentration (X2) and Co-SAA amount (X3) were the most dominant significant factors with the highest co-efficient estimates.

This finding could be explained as ζ-potential measures the charges on the surface of the particles,[46] and increasing the concentration of X2 and X3 resulted in high coverage of the surface of GCBE-SLNs, which reduced the electrophoretic mobility of the nanoparticles and subsequently decreased the ζ-potential.[37] Correspondingly, their higher-order terms ($X2^2$ and $X3^2$) also showed significant indirect relationships with ζ-potential. Results also indicated that the increased interaction between surfactant concentration and Co-SAA amount (X2X3) led to a significant reduction in ζ-potential. This finding may be related to the fact that both factors (X2) and (X3) are responsible for reducing ζ-potential.

According to ANOVA test results (Table 3), lipid concentration (X1) had an antagonistic relationship with ζ-potential. This finding is consistent with the research work conducted by Mendes et al.,[47] which reported that the ζ-potential decreases while the particle size increases by increasing the phospholipid concentration due to the decreased available surface area charge, which is also consistent with our particle size results.

Influence of Investigated Parameters on Entrapment Efficiency (EE%) (Y4). When it comes to nano-therapeutics, an ideal therapeutic payload is required to ensure adequate drug delivery to the target region. As a result, fine-tuning different formulations and processing parameters to achieve adequate entrapment of the drug is a severe concern to researchers. The GCBE absorption spectrum using the UV−vis spectrophotometer and standard calibration curve are demonstrated in Figures S1 and S2, respectively. In the current study, the designed SLNs seemed to have reasonable EE% reaching 68.2 ± 2.35%.

As evidenced by the ANOVA test results (Table 3), lipid concentration (X1) synergistically influenced entrapment efficiency. This finding can be interpreted that the increase in lipid content offering an additional capacity to incorporate an extra drug amount during the preparation of GCBE-SLNs. Moreover, the increase in lipid concentration increased the dispersion viscosity and accelerated the solidification and thus prevented the diffusion of the drug from the inner phase to the aqueous phase, subsequently increasing EE%.[22] This finding agrees with the results obtained by Emami et al.[39]

https://doi.org/10.1021/acsomega.2c06629
ACS Omega 2023, 8, 20251−20261

Furthermore, this finding was highly correlated with those of particle size. Principally, the higher the lipid concentration, the more available extra spaces for the drug; thus, the larger yielded particle size and higher EE.

In contrast, as demonstrated in the 3D surface plot (Figure 2), surfactant concentration (X2) showed a significant indirect impact on EE% (p-value = 0.0204). This finding was consistent with Emami et al.,[39] who stated that the increase in the surfactant concentration reduced the entrapment efficiency. This finding could be ascribed to increasing the drug solubility in the aqueous phase as a consequence of increasing the surfactant concentration due to the emulsifier's solubilization effect. In addition, part of the GCBE was loaded in the surfactant layer at the GCBE-SLNs surface, resulting in lower drug entrapment.[39,48]

In contrast, results revealed that Co-SAA amount (X3) had a significant positive influence on entrapment efficiency (Y3), which could be explained by increasing the solubility of the drug in the lipid, which enhanced the entrapment efficiency of the drug.[49]

Influence of Investigated Parameters on Cumulative Drug Release (Y5). Cumulative drug released from prepared SLNs ranged from 46.0 ± 7.80 to 100.0 ± 3.54%. It is evident from Figure 1 that cumulative drug release of GCBE-loaded SLNs demonstrated a biphasic release, including an initial burst release over the first few hours, followed by a sustained, slow release.[50] This pattern of release is noted in matrix-based formulations such as SLNs, where drug release occurs primarily through lipid matrix diffusion or biodegradation and surface erosion. The initial burst drug release rate is usually caused by drug adsorption on the surface of the particles and particles' solubilization from the outermost layer.[51] The release of a significant amount of drug during this short phase of burst release (more than 50%) may be due to changes in the drug's partition coefficient, which led to the drug's presence on the lipid particles' surface. In addition, the high drug release may be attributed to the large surface area of the nanoparticles. The extended, regulated diffusion of the dissolving medium into the deep matrix layer impacts the solubilization of the drug, which increases the viscosity of the stagnant layer caused by matrix degradation, which results in retarding medium penetration into the matrix and delaying the dissolution process over time,[35] while the non-formulated GCBE solution had a faster rate of release under the same conditions, as almost all the amount of GCBE was released within the first 2 h, as demonstrated in Figure 1.

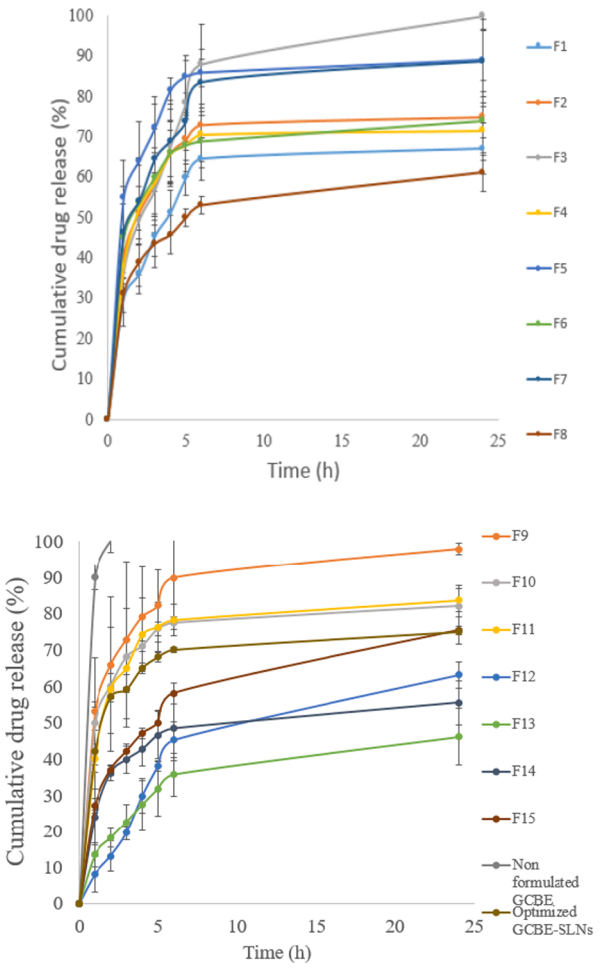

Figure 1. Cumulative drug release of GCBE-SLNs formulations and non-formulated GCBE.

As noticed by the ANOVA test results (Table 3) and 3D surface (Figure 2), lipid concentration (X1) showed a significant indirect influence on drug release (Y5) with a p-value of 0.0065. The decrement in drug release from SLNs accompanied the augmentation of lipid concentration. This finding can be justified as increasing lipid concentration resulted in particle size enlargement and lower surface area of the particles leading to a lower drug release rate, which was highly correlated with the aforementioned findings of particle size. In addition, high lipid concentration results in increased viscosity and rigidity of the SLNs dispersion, which causes slower drug diffusion to the dissolution medium.[37] Moreover, it could be interpreted by the enhanced drug entrapment efficiency upon increasing the lipid concentration, which reduced the drug release from SLNs. This correlated well with the aforementioned findings of EE%.

Regarding surfactant concentration (X2), results illustrated a significant direct relationship between X2 and Y5. This phenomenon may result from increasing the solubilization and drug release from SLNs.[52] Comparable findings were reported by Khalil et al.,[53] who noted that the increase in surfactant concentration from 0.5 to 5% w/w increased the cumulative release of meloxicam from SLNs. In addition, Gidwani and Vyas also supported the above-mentioned explanation and added that the concentrations of the lipid and the surfactant greatly influence the rate of initial burst drug release. High surfactant concentration resulted in a higher initial drug burst release rate, leading to higher cumulative drug release. On the other hand, higher lipid concentration resulted in a lower burst release rate as a higher amount of the drug was present in the lipid core,[54] which is in agreement with the results obtained by our study.

Moreover, the drug amount partitioning to the aqueous phase increases with high surfactant concentration, increasing the rate and amount of drug released.[55] Moreover, increasing surfactant concentration may lead to a higher drug release rate as it decreases the interfacial tension between the nanoparticles and the medium, resulting in reducing the drug aggregations and increasing the drug dissolution rate.[56] Our findings agreed with Mohtar et al.[52] and Gao et al.[57] Furthermore, the amount of Co-SAA showed an insignificant direct relationship with drug release, which could be explained as propylene glycol acts as a penetration enhancer, so increasing its amount may

https://doi.org/10.1021/acsomega.2c06629
ACS Omega 2023, 8, 20251−20261

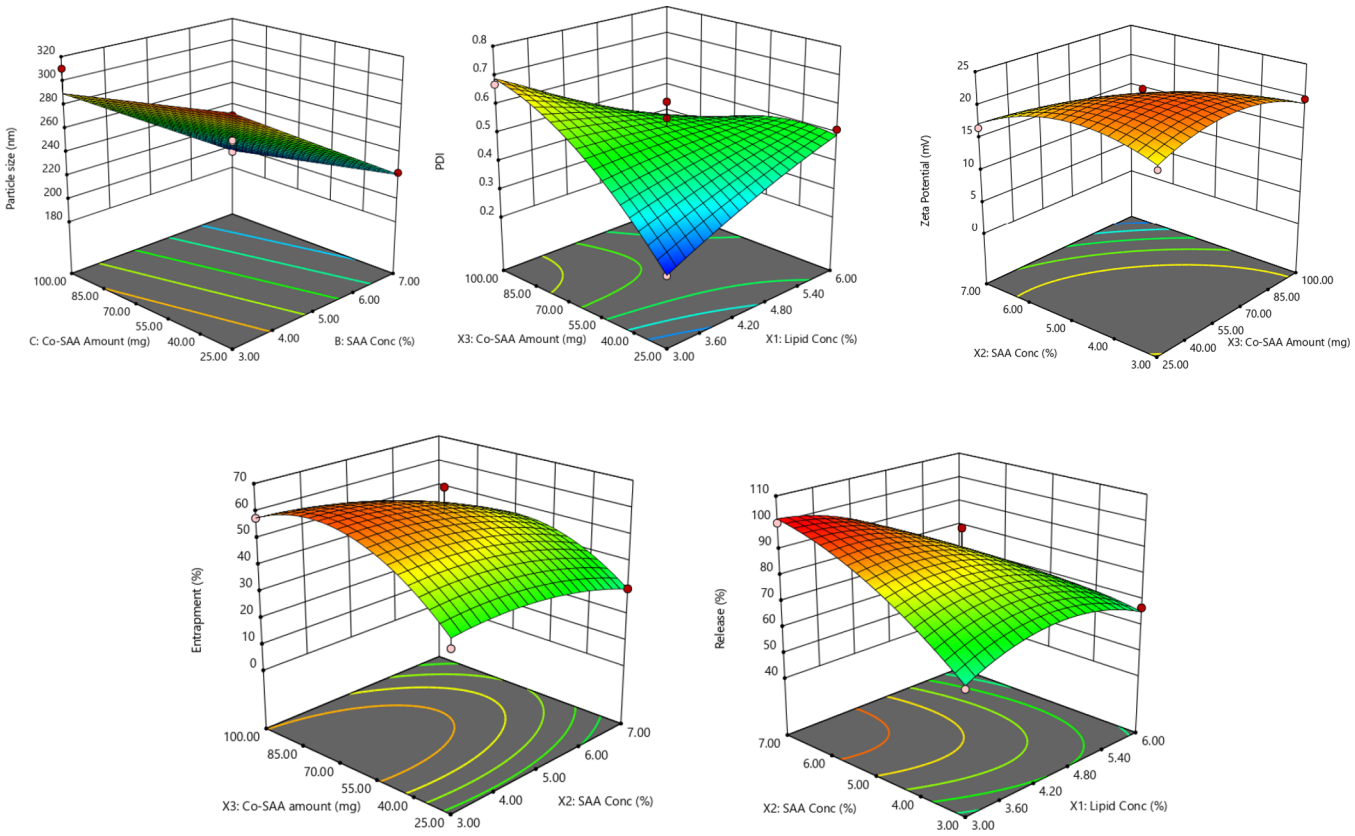

Figure 2. 3D surface plot of particle size, PDI, ζ-potential, entrapment %, and release %.

enhance the release of drugs from SLNs.[58,59] The kinetic release pattern was best fitted by the Higuchi model, which was consistent with Yasir and Sara,[60] who reported that the Higuchi kinetic model best described the release of haloperidol from SLNs.

Mathematical Models for Responses.

$$\text{Particle size (Y1)} = +255.67 + 9.26X1 - 46.71X2 - 12.55X3 \quad (2)$$

$$\text{PDI (Y2)} = +0.5273 - 0.0369X1 + 0.0071X2 + 0.0610X3 - 0.1237X1X2 - 0.1610X1X3 - 0.0395X2X3 - 0.0178X1^2 + 0.0682X2^2 - 0.0785X3^2 \quad (3)$$

$$\zeta - \text{Potential (Y3)} = +21.27 - 1.27X1 - 4.19X2 - 3.29X3 + 0.6250X1X2 + 0.9125X1X3 - 3.15X2X3 - 0.2771X1^2 - 3.26X2^2 - 3.00X3^2 \quad (4)$$

$$\text{Entrapment efficiency\%(Y4)} = +58.77 + 4.11X1 - 7.56X2 + 6.34X3 + 19.13X1X2 + 10.12X1X3 - 3.19X2X3 - 12.39X1^2 - 4.44X2^2 - 13.80X3^2 \quad (5)$$

$$\text{Cumulative drug release\%(Y5)} = +87.82 - 10.12X1 + 7.94X2 + 0.8538X3 - 10.71X1X2 + 9.80X1X3 + 8.73X2X3 - 9.09X1^2 - 5.94X2^2 - 8.46X3^2 \quad (6)$$

Development of the Optimized GCBE-Loaded SLN Formulas. Analyses of the experimental factors were carried out to study the examined responses to predict the levels of factors that exert optimum combination, which maximizes the desirability function and identifies the best-performing GCBE-SLNs, according to the criteria mentioned in Table 1. The optimized formula comprises 5.8% geleol, 5.9% tween 80, and 80.4 mg PG. The predicted and observed responses and standard error of prediction are shown in Table 4. Predicted values of optimized formula responses were compared with the

Table 4. Responses of Optimized GCBE-SLNs and the Standard Error of Prediction[a]

responses	predicted values	observation[b]	SD
Y_1: particle size (nm)	235.9	235.7 ± 12.5[c]	0.2
Y_2: PDI	0.388	0.417 ± 0.023[c]	−0.029
Y_3:ζ-potential (mV)	−15	−15 ± 0.14[c]	0
Y_4: entrapment efficiency (%)	59.64	58.3 ± 0.85[c]	1.34
Y_5: cumulative drug release (%)	75	75 ± 0.78[c]	0

[a]Note: standard error of prediction = predicted value − observed value; SD, standard error of prediction. [b]Values are expressed as average ± SD (n = 3). [c]Difference from the predicted values is insignificant (p-value >0.05).

https://doi.org/10.1021/acsomega.2c06629
ACS Omega 2023, 8, 20251−20261

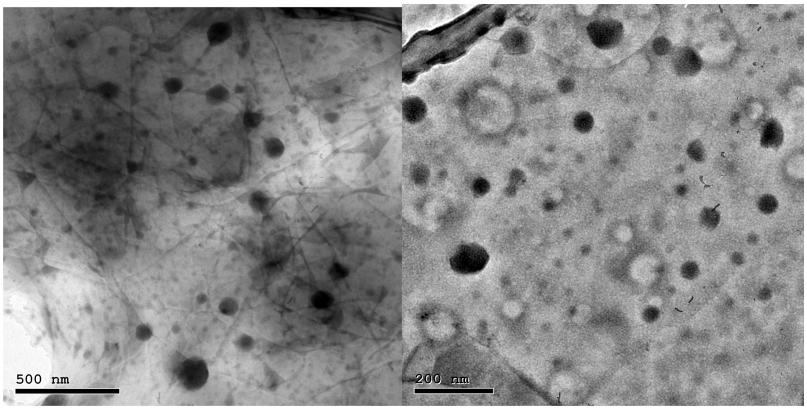

Figure 3. TEM images of optimized GCBE-SLNs.

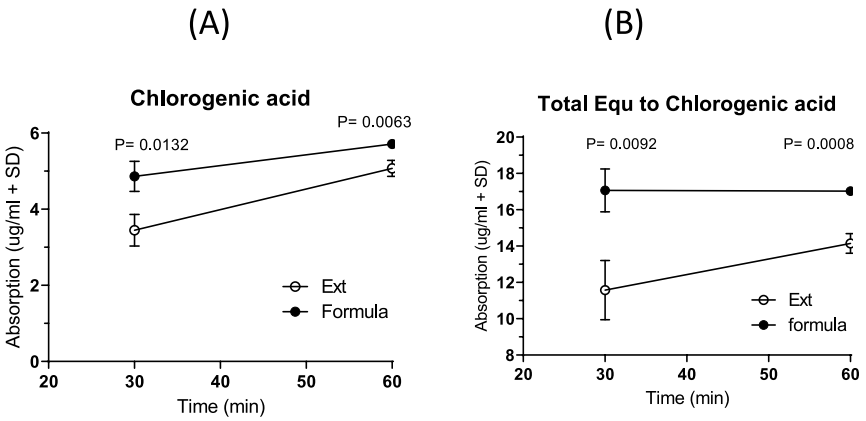

Figure 4. Intestinal absorption of chlorogenic acid (a) and total equivalent to chlorogenic acid (b) from everted gut sac containing optimized GCBE-SLNs formula and non-formulated GCBE.

observed experimental values. The differences between predicted and observed values of particle size, PDI, ζ-potential, entrapment efficiency, and cumulative drug release were insignificant. The achieved desirability was 0.853, which proved the suitability of predicted desirability for responses.[22] In light of these findings, it is likely to conclude that the optimal combination of the independent factors attained the desired characteristics. Thus, the optimized GCBE-SLN formulas were subjected to further assessment studies.

Transmission Electron Microscope (TEM). The TEM microscopic examination was performed to get more insight into the morphology of the optimized GCBE-SLNs. The TEM images (Figures 3 and S3) showed spherically shaped nanoparticles with a reasonably fair distribution consistent with the obtained PDI results of the optimized formula (0.417 ± 0.023). Internalization and drug release are greatly influenced by the shape of nanoparticles (spherical, cubic, rods, and plates). Several studies found that spherical nanoparticles were best suited for drug delivery since they could be absorbed more easily and quickly than rod-shaped nanoparticles.[61]

Ex Vivo Intestinal Permeation Study on Optimized GCBE-SLNs Using the Everted Gut Sac Model. Intestinal permeability means the ability of a substance to penetrate the intestinal epithelium, which is determined mainly by the substance's solubility, size, and charge.[62] The everted gut sac method is an effective model for many intestinal permeability investigations, including in vitro drug absorption mechanisms, efflux transport, and the effect of efflux transport modulators on drug absorption, in addition to drug interactions and multidrug resistance.[63] This model efficiency is due to the presence of a mucus layer and the relatively large surface area available for absorption.

Moreover, the everted gut sac technique results have frequently agreed with their corresponding in vivo observations. However, the main limiting parameter is the viability of tissues. Under physiological conditions, the gut's suggested tissue viability and metabolic activity is 2 h. Different animals were studied for everted gut sac experiments. However, the most frequently used sac for ex vivo studies is the everted rat intestinal sac.[14]

Previous research by Mortelé et al.[13] proved that CGA showed low intestinal absorption with the involvement of an efflux pump. In the current study, the everted gut sac model was used to prove the efficiency of optimized GCBE-SLNs, compared to non-formulated extract (Figure 4), for achieving enhanced intestinal permeation to overcome CGA's low bioavailability.

The percentage of CGA permeated through everted gut sac was measured using the HPLC method. HPLC chromatogram peak of CGA (see the Supporting Information, Figure S4) and the standard calibration curve of CGA were obtained (see the Supporting Information, Figure S5) and the LOD and the LOQ of the HPLC method were 0.2 and 0.25 μg/mL, respectively. The percentages of CGA permeated using GCBE-SLNs were 34.7 and 40.7% after 30 and 60 min, respectively. On the other hand, only 24.57 and 36.2% were permeated using non-formulated extract after 30 and 60 min, respectively.

https://doi.org/10.1021/acsomega.2c06629
ACS Omega 2023, 8, 20251−20261

Figure 4A represents the intestinal absorption of CGA (the main detected compound) from GCBE-SLNs and non-formulated GCBE after 30 and 60 min. Results proved that the permeability of GCBE-SLNs was significantly greater than non-formulated GCBE with *p*-values of 0.0132 and 0.0063 at 30 and 60 min, respectively. In addition, calculating the total peaks equivalent to chlorogenic that may lead to a synergistic effect after use found that the total amount absorbed equivalent to CGA from GCBE-SLNs was significantly higher than that absorbed from non-formulated GCBE (Figure 4B).

This finding is consistent with Masiiwa and Gadaga,[62] where artesunate-loaded SLNs had a significantly higher permeability than non-formulated artesunate using the everted sac model.

The enhancement in intestinal drug permeability could be ascribed to the nano-size of SLNs, which prolonged drug residence time and increased the contact surface area. The increased surface area enhanced the adhesion of the drug to the gut mucosal layer and facilitated drug penetration into the intervillous region, resulting in an improved drug diffusion rate.[51,64] Furthermore, particle size reduction can result in increased dissolution and saturation solubility, which increases the concentration gradient between the intestinal epithelial cells and the underlying mesenteric circulation, resulting in enhanced drug absorption due to the diffusion of SLNs through the mucous layer.[51] Moreover, the surfactant utilized in SLNs formulation may also have contributed to the increased permeability as surfactants can modify membrane fluidity, resulting in enhanced drug absorption through the gut.[62] Furthermore, geleol, being high carbon chain length lipid, also had a vital role in increasing the drug permeability into the intestine. As generally, lipid nanoparticles containing high carbon chains have less susceptibility to intestinal lipase than those composed of a shorter carbon chain and are preferably transported into the intestinal lymphatic system.[65] This finding is in agreement with Pandey et al., who reported that the lipid structure of SLNs makes it suitable and interesting for the oral route of administration to increase the bioavailability by protecting the drug from chemical as well as enzymatic degradation, thereby delaying the in vivo metabolism.[66] The aforementioned findings suggest that the SLNs have a vital role in increasing GCBE intestinal permeability, resulting in improved oral bioavailability, thus confirming our hypothesis.

CONCLUSIONS

GCBE-SLNs were successfully developed using a hot homogenization technique. During the preparation of promising GCBE-loaded SLNs, the influence of lipid concentration, surfactant concentration, and co-surfactant amount on different responses was clarified using BBD by implementing statistical analysis on the formulation responses. It was concluded that the particle size (Y1) and entrapment efficiency (Y4) were highly affected by surfactant concentration and Co-SAA amount. On the other hand, cumulative drug release (Y5) was highly influenced by lipid concentration and surfactant concentration. Moreover, results concluded that the optimum composition of GCBE-SLNs was 5.8% geleol, 5.9% tween 80, and 80.4 mg PG, which was successfully produced with a small particle size of 235.7 ± 12.5 nm. The permeation study performed using everted gut sac verified that loading GCBE in SLNs significantly improved their intestinal permeation compared to non-formulated GCBE. Conclusively, the current work highlights the promising use of oral GCBE-SLNs to enhance the intestinal absorption of CGA to be used in future in vivo studies.

ASSOCIATED CONTENT

Supporting Information

The Supporting Information is available free of charge at https://pubs.acs.org/doi/10.1021/acsomega.2c06629.

Green coffee bean extract absorption spectrum using the UV−vis spectrophotometer, UV−vis spectrophotometer standard calibration curve of GCBE at 324 nm, TEM images of optimized formula of GCBE-SLNs, HPLC chromatogram peak of chlorogenic acid, and the HPLC standard calibration curve of chlorogenic acid (PDF)

AUTHOR INFORMATION

Corresponding Author

Dalia Attia − *Department of Pharmaceutics and Pharmaceutical Technology, Faculty of Pharmacy, The British University in Egypt (BUE), 11837 El-Sherouk City, Cairo, Egypt*; orcid.org/0000-0002-6352-582X; Email: Dalia.rhman@bue.edu.eg

Authors

Yomna A. Moussa − *Department of Pharmaceutics and Pharmaceutical Technology, Faculty of Pharmacy, The British University in Egypt (BUE), 11837 El-Sherouk City, Cairo, Egypt*

Mahmoud H. Teaima − *Department of Pharmaceutics and Industrial Pharmacy, Faculty of Pharmacy, Cairo University, 11562 Cairo, Egypt*

Mohey M. Elmazar − *Department of Pharmacology and Toxicology, Faculty of Pharmacy, The British University in Egypt (BUE), 11837 El-Sherouk City, Cairo, Egypt*

Mohamed A. El-Nabarawi − *Department of Pharmaceutics and Industrial Pharmacy, Faculty of Pharmacy, Cairo University, 11562 Cairo, Egypt*

Complete contact information is available at: https://pubs.acs.org/10.1021/acsomega.2c06629

Notes

The authors declare no competing financial interest.

ACKNOWLEDGMENTS

The authors would like to express their gratitude to Dr. Khaled A. Nematallah (Faculty of Pharmacy, The British University in Egypt) for his help during this research. The authors also extend their gratitude to Dr. Moataz Sobhy and Dr. Rawda (Faculty of Pharmacy, The British University in Egypt) for their kind help and support during the research work.

REFERENCES

(1) Masek, A.; Latos-Brozio, M.; Kałuzna-Czaplińska, J.; Rosiak, A.; Chrzescijanska, E. Antioxidant Properties of Green Coffee Extract. *Forests* **2020**, *11*, 557.

(2) Onakpoya, I.; Terry, R.; Ernst, E. The Use of Green Coffee Extract as a Weight Loss Supplement: A Systematic Review and Meta-Analysis of Randomised Clinical Trials. *Gastroenterol. Res. Pract.* **2011**, *2011*, No. 382852.

(3) Amigo-Benavent, M.; Wang, S.; Mateos, R.; Sarriá, B.; Bravo, L. Antiproliferative and Cytotoxic Effects of Green Coffee and Yerba Mate Extracts, Their Main Hydroxycinnamic Acids, Methylxanthine and Metabolites in Different Human Cell Lines. *Food Chem. Toxicol.* **2017**, *106*, 125−138.

(4) Khojah, E. Y. Effect of Arabic and Green Coffee Beans on Lowering Lipid Profile Parameters in Male Rats. *Aust. J. Basic Appl. Sci.* **2016**, *10*, 310−317.
(5) Asbaghi, O.; Sadeghian, M.; Nasiri, M.; Khodadost, M.; Shokri, A.; Panahande, B.; Pirouzi, A.; Sadeghi, O. The Effects of Green Coffee Extract Supplementation on Glycemic Indices and Lipid Profile in Adults: A Systematic Review and Dose-Response Meta-Analysis of Clinical Trials. *Nutr. J.* **2020**, *19*, 71.
(6) Singh, B.; Bodla, R. B.; Kumar, A.; Khatri, M. Green Coffee in Pharmaceutical Industry: A Boon To Mankind. *Int. J. Innov. Sci. Eng. Technol.* **2020**, *7*, 149−165.
(7) Cho, A. S.; Jeon, S. M.; Kim, M. J.; Yeo, J.; Seo, K. I.; Choi, M. S.; Lee, M. K. Chlorogenic Acid Exhibits Anti-Obesity Property and Improves Lipid Metabolism in High-Fat Diet-Induced-Obese Mice. *Food Chem. Toxicol.* **2010**, *48*, 937−943.
(8) Seguido, M. Á.; Tarradas, R. M.; González-Rámila, S.; García-Cordero, J.; Sarriá, B.; Bravo-Clemente, L.; Mateos, R. Sustained Consumption of a Decaffeinated Green Coffee Nutraceutical Has Limited Effects on Phenolic Metabolism and Bioavailability in Overweight/Obese Subjects. *Nutrients* **2022**, *14*, 2445.
(9) Farias-Pereira, R.; Park, C.-S.; Park, Y. Mechanisms of Action of Coffee Bioactive Components on Lipid Metabolism. *Food Sci. Biotechnol.* **2019**, *28*, 1287−1296.
(10) Ilmiawati, C.; Fitri, F.; Rofinda, Z. D.; Reza, M. Green Coffee Extract Modifies Body Weight, Serum Lipids and TNF-α in High-Fat Diet-Induced Obese Rats. *BMC Res. Notes* **2020**, *13*, 208.
(11) Gao, S.; Basu, S.; Yang, G.; Deb, A.; Hu, M. Oral Bioavailability Challenges of Natural Products Used in Cancer Chemoprevention. *Prog. Chem.* **2013**, *25*, 1553−1574.
(12) Feng, Y.; Sun, C.; Yuan, Y.; Zhu, Y.; Wan, J.; Firempong, C. K.; Omari-Siaw, E.; Xu, Y.; Pu, Z.; Yu, J.; Xu, X. Enhanced Oral Bioavailability and in Vivo Antioxidant Activity of Chlorogenic Acid via Liposomal Formulation. *Int. J. Pharm.* **2016**, *501*, 342−349.
(13) Mortelé, O.; Jorissen, J.; Spacova, I.; Lebeer, S.; Van Nuijs, A. L. N.; Hermans, N. Demonstrating the Involvement of an Active Efflux Mechanism in the Intestinal Absorption of Chlorogenic Acid and Quinic Acid Using a Caco-2 Bidirectional Permeability Assay. *Food Funct.* **2021**, *12*, 417−425.
(14) Alam, M. A.; Al-Jenoobi, F. I.; Al-Mohizea, A. M. Everted Gut Sac Model as a Tool in Pharmaceutical Research: Limitations and Applications. *J. Pharm. Pharmacol.* **2012**, *64*, 326−336.
(15) Chandrakala, V.; Aruna, V.; Angajala, G. Review on Metal Nanoparticles as Nanocarriers: Current Challenges and Perspectives in Drug Delivery Systems. *Emergent Mater.* **2022**, *5*, 1593−1615.
(16) Khater, D.; Nsairat, H.; Odeh, F.; Saleh, M.; Jaber, A.; Alshaer, W.; Al Bawab, A.; Mubarak, M. S. Design, Preparation, and Characterization of Effective Dermal and Transdermal Lipid Nanoparticles: A Review. *Cosmetics* **2021**, *8*, 39.
(17) Doost, A. S.; Nasrabadi, M. N.; Kassozi, V.; Nakisozi, H.; Van der Meeren, P. Recent Advances in Food Colloidal Delivery Systems for Essential Oils and Their Main Components. *Trends Food Sci. Technol.* **2020**, *99*, 474−486.
(18) Gunasekaran, T.; Haile, T.; Nigusse, T.; Dhanaraju, M. D. Nanotechnology: An Effective Tool for Enhancing Bioavailability and Bioactivity of Phytomedicine. *Asian Pac. J. Trop. Biomed.* **2014**, *4*, S1−S7.
(19) Hashem, F.; Nasr, M.; Ahmed, Y. Preparation and Evaluation of Iron Oxide Nanoparticles for Treatment of Iron Deficiency Anemia. *Int. J. Pharm. Pharm. Sci.* **2018**, *10*, 142.
(20) Katopodi, A.; Detsi, A. Solid Lipid Nanoparticles and Nanostructured Lipid Carriers of Natural Products as Promising Systems for Their Bioactivity Enhancement: The Case of Essential Oils and Flavonoids. *Colloids Surf. A Physicochem. Eng. Asp.* **2021**, *630*, No. 127529.
(21) Lin, C. H.; Chen, C. H.; Lin, Z. C.; Fang, J. Y. Recent Advances in Oral Delivery of Drugs and Bioactive Natural Products Using Solid Lipid Nanoparticles as the Carriers. *J. Food Drug Anal.* **2017**, *25*, 219−234.
(22) Patel, M.; Sawant, K. A Quality by Design Concept on Lipid Based Nanoformulation Containing Antipsychotic Drug: Screening Design and Optimization Using Response Surface Methodology. *J. Text. Sci. Eng.* **2017**, *08*, 442.
(23) Yeganeh, E. M.; Bagheri, H.; Mahjub, R. Preparation, Statistical Optimization and in-Vitro Characterization of a Dry Powder Inhaler (Dpi) Containing Solid Lipid Nanoparticles Encapsulating Amphotericin b: Ion Paired Complexes with Distearoyl Phosphatidylglycerol. *Iran. J. Pharm. Res.* **2020**, *19*, 45−62.
(24) Garms, B. C.; Poli, H.; Baggley, D.; Han, F. Y.; Whittaker, A. K.; Anitha, A.; Grøndahl, L. Evaluating the Effect of Synthesis, Isolation, and Characterisation Variables on Reported Particle Size and Dispersity of Drug Loaded PLGA Nanoparticles. *Mater. Adv.* **2021**, *2*, 5657−5671.
(25) Paswan, S. K.; Saini, T. R. Comparative Evaluation of in Vitro Drug Release Methods Employed for Nanoparticle Drug Release Studies. *Dissolution Technol.* **2021**, *28*, 30−38.
(26) Moscardini, A.; Di Pietro, S.; Signore, G.; Parlanti, P.; Santi, M.; Gemmi, M.; Cappello, V. Uranium-Free X Solution: A New Generation Contrast Agent for Biological Samples Ultrastructure. *Sci. Rep.* **2020**, *10*, 11540.
(27) Nematallah, K. A.; Elmekkawy, S.; Abdollah, M. R. A.; Elmazar, M. M.; Abdel-Sattar, E.; Meselhy, M. R. Cheminformatics Application in the Phytochemical and Biological Study of Eucalyptus Globulus L. Bark as a Potential Hepatoprotective Drug. *ACS Omega* **2022**, *7*, 7945−7956.
(28) Schilling, R. J.; Mitra, A. K. Intestinal Mucosal Transport of Insulin. *Int. J. Pharm.* **1990**, *62*, 53−64.
(29) Parsa, A.; Saadati, R.; Abbasian, Z.; Aramaki, S. A.; Dadashzadeh, S. Enhanced Permeability of Etoposide across Everted Sacs of Rat Small Intestine by Vitamin E-TPGS. *Iran. J. Pharm. Res.* **2013**, *12*, 35−44.
(30) Shan, Y.; Jin, X.; Cheng, Y.; Yan, W. Simultaneous Determination of Chlorogenic Acids in Green Coffee Bean Extracts with Effective Relative Response Factors. *Int. J. Food Prop.* **2017**, *20*, 2028−2040.
(31) Duong, V. A.; Nguyen, T. T. L.; Maeng, H. J. Preparation of Solid Lipid Nanoparticles and Nanostructured Lipid Carriers for Drug Delivery and the Effects of Preparation Parameters of Solvent Injection Method. *Molecules* **2020**, *25*, 4781.
(32) Gupta, B.; Poudel, B. K.; Pathak, S.; Tak, J. W.; Lee, H. H.; Jeong, J. H.; Choi, H. G.; Yong, C. S.; Kim, J. O. Effects of Formulation Variables on the Particle Size and Drug Encapsulation of Imatinib-Loaded Solid Lipid Nanoparticles. *AAPS PharmSciTech* **2016**, *17*, 652−662.
(33) Muhtadi, W. K.; Novitasari, L.; Martien, R.; Danarti, R. Factorial Design as the Method in the Optimization of Timolol Maleate-Loaded Nanoparticle Prepared by Ionic Gelation Technique. *Int. J. Appl. Pharm.* **2019**, *11*, 66−70.
(34) El-Naggar, N. E. A.; Saber, W. E. I. A.; Zweil, A. M.; Bashir, S. I. An Innovative Green Synthesis Approach of Chitosan Nanoparticles and Their Inhibitory Activity against Phytopathogenic Botrytis Cinerea on Strawberry Leaves. *Sci. Rep.* **2022**, *12*, 3515.
(35) Khames, A.; Khaleel, M. A.; El-Badawy, M. F.; El-Nezhawy, A. O. H. Natamycin Solid Lipid Nanoparticles - Sustained Ocular Delivery System of Higher Corneal Penetration against Deep Fungal Keratitis: Preparation and Optimization. *Int. J. Nanomed.* **2019**, *14*, 2515−2531.
(36) Shah, D. Effect Of Lipid And Surfactant Concentration On Cefpodoximeproxetilsolid Lipid Nanoparticle. *Eur. J. Biomed. Pharm. Sci.* **2017**, *4*, 817−823.
(37) Badawi, N. M.; Hteaima, M. H.; El-Say, K. M.; Aattia, D. A.; Ael-Nabarawi, M. A.; Elmazar, M. M. Pomegranate Extract-Loaded Solid Lipid Nanoparticles: Design, Optimization, and in Vitro Cytotoxicity Study. *Int. J. Nanomed.* **2018**, *13*, 1313−1326.
(38) Bhalekar, M.; Upadhaya, P.; Madgulkar, A. Formulation and Characterization of Solid Lipid Nanoparticles for an Anti-Retroviral Drug Darunavir. *Appl. Nanosci.* **2017**, *7*, 47−57.

https://doi.org/10.1021/acsomega.2c06629
ACS Omega 2023, 8, 20251−20261

(39) Emami, J.; Mohiti, H.; Hamishehkar, H.; Varshosaz, J. Formulation and Optimization of Solid Lipid Nanoparticle Formulation for Pulmonary Delivery of Budesonide Using Taguchi and Box-Behnken Design. *Res. Pharm. Sci.* **2015**, *10*, 17−33.
(40) Badawi, N.; El-Say, K.; Attia, D.; El-Nabarawi, M.; Elmazar, M.; Teaima, M. Development of Pomegranate Extract-Loaded Solid Lipid Nanoparticles: Quality by Design Approach to Screen the Variables Affecting the Quality Attributes and Characterization. *ACS Omega* **2020**, *5*, 21712−21721.
(41) Lamie, C.; Elmowafy, E.; Attia, D. A.; Elmazar, M. M.; Mortada, N. D. Diversifying the Skin Cancer-Fighting Worthwhile Frontiers: How Relevant Are the Itraconazole/Ascorbyl Palmitate Nanovectors? *Nanomed. Nanotechnol. Biol. Med.* **2022**, *43*, No. 102561.
(42) Wang, C.; Cui, B.; Guo, L.; Wang, A.; Zhao, X.; Wang, Y.; Sun, C.; Zeng, Z.; Zhi, H.; Chen, H.; Liu, G.; Cui, H. Fabrication and Evaluation of Lambda-Cyhalothrin Nanosuspension by One-Step Melt Emulsification Technique. *Nanomaterials (Basel)* **2019**, *9*, 145.
(43) Tantra, R.; Schulze, P.; Quincey, P. Effect of Nanoparticle Concentration on Zeta-Potential Measurement Results and Reproducibility. *Particuology* **2010**, *8*, 279−285.
(44) Scioli Montoto, S.; Muraca, G.; Ruiz, M. E. Solid Lipid Nanoparticles for Drug Delivery: Pharmacological and Biopharmaceutical Aspects. *Front. Mol. Biosci.* **2020**, *7*, No. 587997.
(45) Tan, M. E.; He, C. H.; Jiang, W.; Zeng, C.; Yu, N.; Huang, W.; Gao, Z. G.; Xing, J. G. Development of Solid Lipid Nanoparticles Containing Total Flavonoid Extract from Dracocephalum Moldavica L. And Their Therapeutic Effect against Myocardial Ischemia-Reperfusion Injury in Rats. *Int. J. Nanomed.* **2017**, *12*, 3253−3265.
(46) Honary, S.; Zahir, F. Effect of Zeta Potential on the Properties of Nano-Drug Delivery Systems - A Review (Part 2). *Trop. J. Pharm. Res.* **2013**, *12*, 265−273.
(47) Mendes, A. C.; Shekarforoush, E.; Engwer, C.; Beeren, S. R.; Gorzelanny, C.; Goycoolea, F. M.; Chronakis, I. S. Co-Assembly of Chitosan and Phospholipids into Hybrid Hydrogels. *Pure Appl. Chem.* **2016**, *88*, 905−916.
(48) Sharma, N.; Madan, P.; Lin, S. Effect of Process and Formulation Variables on the Preparation of Parenteral Paclitaxel-Loaded Biodegradable Polymeric Nanoparticles: A Co-Surfactant Study. *Asian J. Pharm. Sci.* **2016**, *11*, 404−416.
(49) Tajik, N.; Tajik, M.; Mack, I.; Enck, P. The Potential Effects of Chlorogenic Acid, the Main Phenolic Components in Coffee, on Health: A Comprehensive Review of the Literature. *Eur. J. Nutr.* **2017**, *56*, 2215−2244.
(50) Barbosa, R. d. M.; Ribeiro, L. N. M.; Casadei, B. R.; da Silva, C. M. G.; Queiróz, V. A.; Duran, N.; de Araújo, D. R.; Severino, P.; de Paula, E. Solid Lipid Nanoparticles for Dibucaine Sustained Release. *Pharmaceutics* **2018**, *10*, 231.
(51) Ibrahim, W. M.; AlOmrani, A. H.; Yassin, A. E. Novel Sulpiride-Loaded Solid Lipid Nanoparticles with Enhanced Intestinal Permeability. *Int. J. Nanomed.* **2014**, *9*, 129−144.
(52) Mohtar, N.; Khan, N. A. K.; Darwis, Y. Solid Lipid Nanoparticles of Atovaquone Based on 24full-Factorial Design. *Iran. J. Pharm. Res.* **2015**, *14*, 989−1000.
(53) Khalil, R. M.; El-bary, A. A.; Kassem, M. A.; Ghorab, M. M.; Ahmed, M. B. Solid Lipid Nanoparticles for Topical Delivery of Meloxicam: Development and In Vitro Characterization. *Eur. Sci. J.* **2013**, *4*, 24−26.
(54) Gidwani, B.; Vyas, A. Preparation, Characterization, and Optimization of Altretamine-Loaded Solid Lipid Nanoparticles Using Box-Behnken Design and Response Surface Methodology. *Artif. Cells Nanomed. Biotechnol.* **2016**, *44*, 571−580.
(55) Dahlman, P. High Pressure Jet Assistance in Steel Turning. *Doktorsavhandlingar vid Chalmers Tek. Hogsk.* **2005**, *50*, 1−63.
(56) El-Housiny, S.; Eldeen, M. A. S.; El-Attar, Y. A.; Salem, H. A.; Attia, D.; Bendas, E. R.; El-Nabarawi, M. A. Fluconazole-Loaded Solid Lipid Nanoparticles Topical Gel for Treatment of Pityriasis Versicolor: Formulation and Clinical Study. *Drug Deliv.* **2018**, *25*, 78−90.
(57) Gao, L.; Zhang, L.; He, F.; Chen, J.; Zhao, M.; Li, S.; Wu, H.; Liu, Y.; Zhang, Y.; Ping, Q.; Hu, L.; Qiao, H. Surfactant Assisted Rapid-Release Liposomal Strategies Enhance the Antitumor Efficiency of Bufalin Derivative and Reduce Cardiotoxicity. *Int. J. Nanomed.* **2021**, *16*, 3581−3598.
(58) Abdel Salam, L.; Abdelmottaleb, M.; Geneidi, A. Formulation and Characterization of Proniosomal Gels Loaded with Levofloxacin for Dermal Drug Delivery. *Arch. Pharm. Sci. Ain Shams Univ.* **2021**, *5*, 288−303.
(59) Shah, S. N. H.; Tahir, M. A.; Safdar, A.; Riaz, R.; Shahzad, Y.; Rabbani, M.; Karim, S.; Murtaza, G. Effect of Permeation Enhancers on the Release Behavior and Permeation Kinetics of Novel Tramadol Lotions. *Trop. J. Pharm. Res.* **2013**, *12*, 27−32.
(60) Yasir, M.; Sara, U. V. S. Solid Lipid Nanoparticles for Nose to Brain Delivery of Haloperidol: In Vitro Drug Release and Pharmacokinetics Evaluation. *Acta Pharm. Sin. B* **2014**, *4*, 454−463.
(61) Deng, H.; Dutta, P.; Liu, J. Entry Modes of Ellipsoidal Nanoparticles on a Membrane during Clathrin-Mediated Endocytosis. *Soft Matter* **2019**, *15*, 5128−5137.
(62) Masiiwa, W. L.; Gadaga, L. L. Intestinal Permeability of Artesunate-Loaded Solid Lipid Nanoparticles Using the Everted Gut Method. *J. Drug Deliv.* **2018**, *2018*, No. 3021738.
(63) Kumar, A.; Ahuja, A.; Ali, J.; Baboota, S. Curcumin-Loaded Lipid Nanocarrier for Improving Bioavailability, Stability and Cytotoxicity against Malignant Glioma Cells. *Drug Deliv.* **2016**, *23*, 214−229.
(64) Zakeri-Milani, P.; Islambulchilar, Z.; Majidpour, F.; Jannatabadi, E.; Lotfpour, F.; Valizadeh, H. A Study on Enhanced Intestinal Permeability of Clarithromycin Nanoparticles. *Braz. J. Pharm. Sci.* **2014**, *50*, 121−129.
(65) Truzzi, E.; Bongio, C.; Sacchetti, F.; Maretti, E.; Montanari, M.; Iannuccelli, V.; Vismara, E.; Leo, E. Self-Assembled Lipid Nanoparticles for Oral Delivery of Heparin-Coated Iron Oxide Nanoparticles for Theranostic Purposes. *Molecules* **2017**, *22*, 963.
(66) Pandey, S.; Shaikh, F.; Gupta, A.; Tripathi, P.; Yadav, J. S. A Recent Update: Solid Lipid Nanoparticles for Effective Drug Delivery. *Adv. Pharm. Bull.* **2022**, *12*, 17−33.

https://doi.org/10.1021/acsomega.2c06629
ACS Omega 2023, 8, 20251−20261